The area disturbance history in this problem was represented by the expression

$$S'(x,t) = S'_i \cos^2[\pi(x/\lambda_t)]\cos^2[(\pi/2)(t/\tau_t)]$$
$$-0.5 \le x/\lambda_t \le 0.5, \qquad 0 \le t/\tau_t \le 1 \quad (42)$$

The initial bump strength is obtained by integrating over x at $t = 0$:

$$B_i = B(0) = \tfrac{1}{2}\bar{p}S'_i\lambda_t \quad (43)$$

For $\bar{M} = 0.15$, 0.3, and 0.45 and for $\Delta B/H_t$ up to 4%, the strengths calculated using Eqs. (41) agreed with the numerical results within ±1% for both right- and left-moving pulses.

Summary

A one-dimensional, linearized theory is presented for the rapid estimation of the properties of pulses generated in constant-area duct flows by events that can be modeled as abrupt and local additions of mass, momentum, or energy. The theory describes pulses by means of volume integrals of pressure or entropy disturbances (termed "strength") and also by length estimates obtained from kinematic considerations. The method is based on first principles and is capable of describing a variety of triggering mechanisms, two of which have been worked out in detail.

An abrupt addition of heat is shown to create two acoustic compression pulses and one entropy pulse, whose strengths are proportional to the amount of heat added. The combined energy of the two acoustic pulses is greater than energy added as heat, compensated for by the fact that the energy disturbance associated with the entropy pulse is negative. An abrupt, local change of the duct cross-sectional area creates two acoustic pulses, while no entropy pulse is generated. A local, abrupt area reduction creates compression pulses, whereas an area increase yields expansion pulses. The strength of the pulses is proportional to the change of duct volume associated with the wall geometry change.

The analytical predictions are confirmed by experimental data and show excellent agreement with computations performed using two different time-dependent Euler CFD codes.

Acknowledgment

The authors express their sincere thanks to A. B. Opalski for providing the experimental data used in Fig. 2.

References

[1]To, C. W. S., and Doige, A. G., "The Application of a Transient Testing Method to the Determination of Acoustic Properties of Unknown Systems," *Journal of Sound and Vibration*, Vol. 71, No. 4, 1982, pp. 545–554.

[2]Freund, D., and Sajben, M., "Reflection of Large Amplitude Acoustic Pulses from an Axial Flow Compressor," *Journal of Propulsion and Power*, Vol. 16, No. 3, 2000, pp. 406–414.

[3]Opalski, A. B., and Sajben, M., "Inlet/Compressor System Response to Short-Duration Acoustic Disturbances," *Journal of Propulsion and Power*, Vol. 18, No. 4, 2002, pp. 922–932.

[4]Freund, D., and Sajben, M., "Compressor-Face Boundary Condition Experiment: Generation of Acoustic Pulses in Annular Ducts," AIAA Paper 96-2657, July 1996.

[5]Opalski, A. B., and Sajben, M., "High Speed Inlet/Compressor System Response to Short-Duration Acoustic and Entropy Disturbances," AIAA Paper 2002-0372, Jan. 2002.

[6]Atassi, H. M., "Unsteady Aerodynamics of Vortical Flows: Early and Recent Developments," *Aerodynamics and Aeroacoustics*, edited by K. Y. Fung, Advanced Series on Fluid Mechanics, World Scientific Publishing, River Edge, NJ, 1994, pp. 121–171.

[7]Opalski, A. B., "Experimental Investigation of Rapid Flow Transients in an Inlet/Compressor System, Induced by Short-Duration Acoustic and Entropy Disturbances," Ph.D. Dissertation, Dept. of Aerospace Engineering and Engineering Mechanics, Univ. of Cincinnati, Cincinnati, OH, May 2002.

[8]Paynter, G. C., Clark, L. T., and Cole, G. L., "Modeling the Response from a Cascade to an Upstream Acoustic Disturbance," *AIAA Journal*, Vol. 38, No. 8, 2000, pp. 1322–1330.

H. M. Atassi
Associate Editor

Vortex Shedding and Transition Frequencies Associated with Flow Around a Circular Cylinder

N. A. Ahmed* and D. J. Wagner†
University of New South Wales,
Sydney, New South Wales 2052, Australia

Nomenclature

D	=	diameter of circular cylinder
f_s, f_V	=	shear-layer frequency and vortex-shedding frequency
Re	=	Reynolds number
Sr	=	Strouhal number
U_∞, U_{sep}	=	velocity of freestream and velocity at separation
u_{rms}	=	rms velocity
v	=	kinematic viscosity
x, y	=	coordinates of a Cartesian system
δ_x	=	displacement thickness

Introduction

FLOW around a circular cylinder has been studied for a long time,[1] and yet our knowledge, at best, is empirical. Of particular interest is the relationship between the ways that the Strouhal number varies with the Reynolds number for a circular cylinder flow. Above a Reynolds number of 10^3, transition to turbulence occurs in a separating shear layer, which is closely tied to the generation of large-scale vortices. Bloor[2] measured the frequency of transition waves within $1.3 \times 10^3 < Re < 4.5 \times 10^4$ and attempted theoretically to derive the relationship between the ratio of the shear-layer transition frequency and the main vortex-shedding frequency. She argued that $f_s/f_V \propto Re^{0.5}$ within $4 \times 10^2 < Re < 2.5 \times 10^5$. Although some experimental results[2,3] fit this prediction well, others[4,5] do not. The purpose of this Note is, therefore, to revisit the preceding problem by observing the dominant frequencies in the transition Reynolds-number range.

Experiment

The 18 × 18 in. open-circuit wind tunnel[6] of the aerodynamic laboratory of the University of New South Wales was used. The experimental setup is shown in Fig. 1. The velocity of the wind tunnel was found to be uniform to within ±0.2% and a turbulence intensity of less than 0.2%. These figures were taken to indicate low acoustic errors associated with the tunnel. The speed of the wind tunnel could be varied between 0 and 25 m/s. Two hot-wire signals were sampled simultaneously, one to take the reading at a point and the other to act as a reference in phase. Thus one hot wire, buried into the model cylinder surface, was moved around to the different angular locations on the cylinder, keeping the same height above the surface, and another hot wire was traversed through the external field using a traversing mechanism.

Test Model

A circular cylinder of diameter 70 mm, with a recess on the surface of the cylinder, was manufactured. The cylinder itself consisted of three hollowed segments so that it could be assembled and disassembled easily enabling the hot wire to be put in and signal cable

Received 30 July 2001; revision received 11 November 2002; accepted for publication 18 November 2002.

*Senior Lecturer, School of Mechanical and Manufacturing Engineering.
†Graduate Student, School of Mechanical and Manufacturing Engineering.

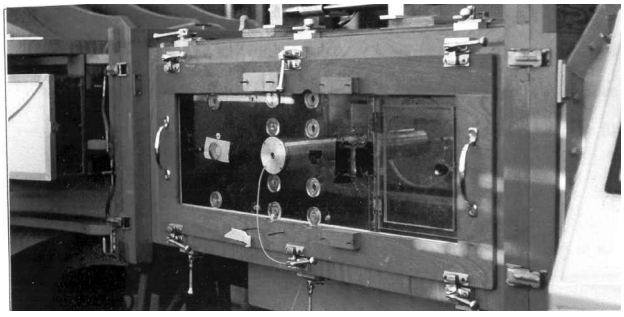

Fig. 1 Experimental setup showing wind-tunnel test section and the test model.

to get out of the cylinder. Thus there was the main part that was used to mount the hot wire, and the other two segments allowed the cylinder to span across the wind-tunnel section. Blockage, end wall,[7] and probe effect are important considerations in studies such as this. The blockage of the test model in relation to the wind tunnel was then around 16.5%. Studies by West and Apelt[8] have shown that a blockage of this magnitude does not affect the nondimensional frequency or Strouhal number of the flow. Limited velocity measurements and smoke flow visualization also suggested little or no changes to flow around one diameter on either side of the cylinder midspan and as a result of the hot-wire probe. It was, therefore, anticipated that the qualitative features of the results presented here would not be significantly affected if measurements were conducted at the center location of the test section.

Data Acquisition and Analysis

Tests were carried out at a sampling rate of 10 kHz, a sweep time of 3 s, and 30,000 points in a sample. A total of 25 samples were obtained for each frequency spectrum. Once transition waves were detected, the repeat tests were carried out with a sampling rate of 20 kHz, a sweep time of 1.5 s, and 30,000 points in a sample. Correction of the mean velocity readings as a result of "rectifying effect" was made in a manner suggested by Kovaszany[9] on the basis of nonlinear hot-wire characteristics with the use of the velocity fluctuations measured at the same point.

The primary tool employed for data analysis of the various signals was the power spectral density. In presenting results the power spectral data have been multiplied by the factor $U_\infty/(u^2_{\text{rms}}D)$, a normalization procedure used by Szepessey and Bearman.[10] The maximum error in Strouhal number was found to be $\pm 0.5\%$ for this study.

Results

Transition waves were detected in the hot-wire signals at several locations within the range of $0.02 < x/D < 0.29$, as quoted by Bloor.[2] The normalized power spectral density plot also showed the peaks associated with vortex shedding and transition frequencies. But at $x/D = 0.21$, $y/D = 0.61$, and $Re = 4.5 \times 10^4$, the hot-wire signals picked up the distinctive features associated with transition waves (Fig. 2a). However, the normalized power spectral density plot (Fig. 2b), in addition to the vortex-shedding frequency peak, also showed two peaks associated with transition frequency, something not observed by other workers in the separated shear layer of a circular cylinder. Experiments were further carried out at three other different Reynolds numbers within the expected transition region. Once gain, two peaks were also observed at $x/D = 0.23$ and $y/D = 0.64$ for $Re = 2.9 \times 10^4$ and at $x/D = 0.26$ and $y/D = 0.61$ for $Re = 3.3 \times 10^4$. At $x/D = 0.16$ and $y/D = 0.61$ for $Re = 9.7 \times 10^4$, however, only one peak associated with transition frequency was found.

Discussion

The existence of two peaks associated with transition frequencies might suggest that the transition point is nonstationary and oscillating or that there are two modes of transition that occur in the separated shear layer of the circular cylinder, one governed by the boundary-layer thickness of the boundary layer, as suggested by Bloor,[2] leading to the $Re^{1/2}$ relationship, and the other governed by

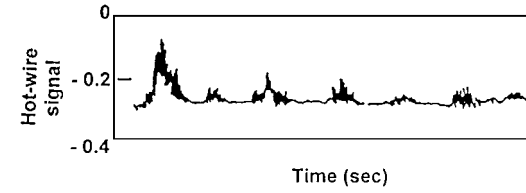

Fig. 2a Hot-wire signal showing evidence of transition waves.

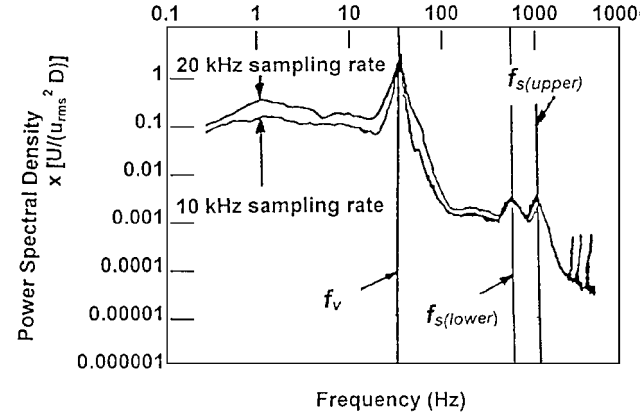

Fig. 2b Power spectral density showing vortex-shedding peak and two transition peaks at 20- and 10-kHz sampling rates (at $x/D = 0.21$, $y/D = 0.61$, and $Re = 4.5 \times 10^5$).

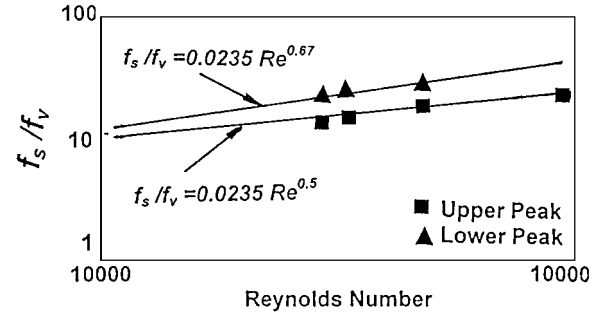

Fig. 3 Variation of upper and lower transition frequency ratios with Reynolds numbers.

the momentum thickness of the shear layer. Consequently Fig. 3, which has two lines drawn according to the empirically obtained relationships[4,5] of $0.095 \times Re^{0.5}$ and $0.0235 \times Re^{0.67}$, respectively, was produced, and the results of the present study were superimposed. It can be seen that the data corresponding to the first or lower peak of transition resemble somewhat the $Re^{0.5}$ relationship, whereas the data from the second peak fit the $Re^{0.67}$ relationship very well.

A further examination of the magnitude of the first and second peaks associated with transition frequencies reveals that the second peak has a magnitude that is approximately twice the first. This raises the possibility that they might be the subharmonic of the transition frequencies in the separated shear layer of a circular cylinder.[11,12] However, Unal and Rockwell[13] found no sign of subharmonics of the transition frequencies within the separated shear layer. Interestingly, when a splitter plate was present, Unal and Rockwell observed subharmonics appearing.

Conclusions

It appears entirely plausible that the two peaks observed in this study are the main transition frequency and its subharmonic. In addition, the readings of the present investigation were at a Reynolds number that is at a higher end of the transition region as suggested by Bloor,[2] giving plenty of time for the amplication of the subharmonic to occur.

References

[1] Strouhal, V., "Uber eine Besondere Art der Tonnerrgung," *Annual Review of Physics and Chemistry*, New Series 5, 1878, pp. 216–251.

[2]Bloor, S., "The Transition to Turbulence in the Wake of a Circular Cylinder," *Journal of Fluid Mechanics*, Vol. 19, 1963, pp. 290–303.

[3]Koutra, A., Boisson, H. C., Chassaing, P., and Ha Minh, H., "Non Linear Interaction and the Transition to Turbulence in the Wake of a Circular Cylinder," *Journal of Fluid Mechanics*, Vol. 181, 1987, pp. 141–161.

[4]Wei, T., and Smith, C. R., "Secondary Vortices in the Wake of Circular Cylinders," *Journal of Fluid Mechanics*, Vol. 169, 1986, pp. 513–533.

[5]Prasad, A., and Williamson, C. H. K., "The Instability of the Shear Layer Separating from a Bluff Body," *Journal of Fluid Mechanics*, Vol. 333, 1997, pp. 375–402.

[6]Ahmed, N. A., and Archer, R. D., "Post-Stall Behavior of a Wing Under Externally Imposed Sound," *Journal of Aircraft*, Vol. 38, No. 5, 2001, pp. 961–963.

[7]Gatto, A., Ahmed, N. A., and Archer, R. D., "Investigation of the Upstream End Effect of the Flow Characteristics of a Yawed Circular Cylinder," *Aeronautical Journal of the Royal Aeronautical Society*, Vol. 104, No. 1033, 2000, pp. 125–128.

[8]West, G. S., and Apelt, C. J., "The Effects of Tunnel Blockage and Aspect Ratio on the Mean Flow past a Circular Cylinder with Reynolds Number Between 10^4 and 10^5," *Journal of Fluid Mechanics*, Vol. 114, 1982, pp. 361–377.

[9]Kovasznay, L. S. G., "Hot Wire Investigation of the Wake Behind Cylinders at Low Reynolds Numbers," *Proceedings of the Royal Society of London, Series A*, Vol. 198, July–Sept. 1949, pp. 174–190.

[10]Szepessey, S., and Bearman, P. W., "Aspect Ratio and End Plate Effects on Vortex Shedding from a Circular Cylinder," *Journal of Fluid Mechanics*, Vol. 234, 1992, pp. 191–217.

[11]Ho, C. H., and Huerre, P., "Perturbed Free Shear Layers," *Annual Review of Fluid Mechanics*, Vol. 16, 1984, pp. 365–424.

[12]Roshko, A., "Structure of Turbulent Shear Flows: A New Look," *AIAA Journal*, Vol. 14, No. 10, 1976, pp. 1349–1357.

[13]Unal, M. F., and Rockwell, D., "On Vortex Formation from a Cylinder. Part 2: The Initial Instability," *Journal of Fluid Mechanics*, Vol. 190, 1988, pp. 513–528.

W. J. Devenport
Associate Editor

Vortex Breakdown–Tail Interaction

Y. Kim,* M. Ozgoren,† and D. Rockwell‡
Lehigh University, Bethlehem, Pennsylvania 18015

Introduction

THE impingement of a broken-down vortex on a tail is part of a larger framework of vortex-body interactions, as reviewed by Rockwell.[1] The buffeting of the tail of an F-series aircraft is well known and has been investigated from a variety of perspectives in recent years. This interaction may be associated with several forms of unsteadiness: nonperiodic displacements of the entire vortex core,[2] a helical-mode instability of the broken-down vortex,[3,4] and streamwise fluctuations of the region of vortex breakdown.[5] A variety of qualitative flow visualizations, usually in conjunction with unsteady loading characteristics of the tail, have been pursued in recent years. Fewer studies, however, have quantitatively addressed the major features of the flow. Beutner et al.[6] determined the rms variations of fluctuating quantities of the flowfield, and Canbazoglu et al.[7,8] provide instantaneous and averaged representations of the flow structure. Related numerical investigations include the works of Rizk and Gee,[9] Gee et al.,[10] Kandil et al.,[11] and Rizzetta.[12] Certain features of the vortex breakdown–tail interaction can be simulated experimentally by vortex encounter with a flat plate having a zero sweep angle, as shown by Wolfe et al.[13] and Mayori and Rockwell.[14] The corresponding computations by Gordnier and Visbal[15] fully accounted for the instantaneous and time-averaged flow structure, in three-dimensional form.

Particularly relevant to the present investigation are the works of Washburn et al.[16] and Canbazoglu et al.[8] Both of these investigations detected not only a primary (incident) vortex along the tail, but also a secondary (counter) vortex that was generally attributable to some type of vortex generation in the leading region of the tail; the physics of the onset of the secondary vortex, however, were not addressed. Although certain aspects of the fluctuating vorticity field were preliminarily characterized by Canbazoglu et al.,[8] the fluctuating velocity fields, which are essential for characterizing the origin of buffet loading of the tail, have not been addressed. Furthermore, the physical origin of these velocity fluctuations is intimately related to the Reynolds stress, which also has not been provided.

The aim of this investigation is to address these unclarified issues and to interpret them physically using a technique of high-image-density particle image velocimetry.

Experimental System and Techniques

Experiments were performed in a large-scale water channel to allow effective imaging of the flow structure. The water channel had a test section that was 5000 mm long, 927 mm wide, and 610 mm deep. The water level was maintained at an elevation of 559 mm. The delta wing–tail system was mounted upside down within a false wall unit to optimize the imaging of the flow structure. The spanwise width between false walls was 510 mm, and the length of these walls was 590 mm.

The dimensions of the delta wing and tail are illustrated in Fig. 1. The wing had a chord C of 342 mm and a thickness-to-chord ratio $t_w/C = 0.028$. The sweep angle of the wing was $\Lambda = 75$ deg. The effective sweep angle of the center of the leading-edge vortex was $\lambda_L = 79$ deg. For all experiments, the angle of attack of the wing was maintained at $\alpha = 21$ deg. The freestream velocity was $U = 152$ mm/s. The Reynolds number based on C was $Re = 5.2 \times 10^4$.

The root chord of the tail was $C_T = 105$ mm; its thickness-to-chord ratio was $t_T/C_T = 0.12$. Both the leading and tip edges of the tail were beveled at an angle of 30 deg. The span of the swept leading edge of the tail was $S_T = 136$ mm, and the angles of inclination

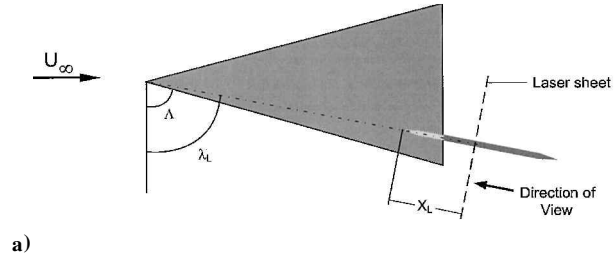

a)

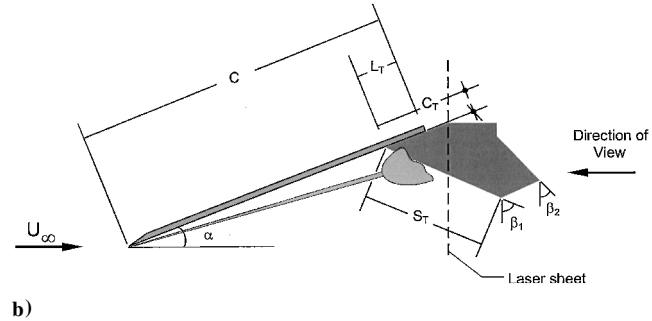

b)

Fig. 1 Schematic of a) plan and b) side views of delta wing–tail arrangement.

Received 19 June 2002; revision received 11 October 2002; accepted for publication 24 October 2002.

*Research Associate, Department of Mechanical Engineering and Mechanics, 354 Packard Laboratory, 19 Memorial Drive West.

†Visiting Scholar, Department of Mechanical Engineering and Mechanics, 354 Packard Laboratory, 19 Memorial Drive West.

‡Paul B. Reinhold Professor, Department of Mechanical Engineering and Mechanics, 354 Packard Laboratory, 19 Memorial Drive West. Member AIAA.